Bull. Chem. Soc. Ethiop. **2024**, 38(4), 937-948.
DOI: https://dx.doi.org/10.4314/bcse.v38i4.10

ISSN 1011-3924
Printed in Ethiopia
Online ISSN 1726-801X

# SYNTHESIS, SPECTROSCOPIC, BIOLOGICAL AND STRUCTURAL CHARACTERIZATIONS FOR THE GOLD(III), PLATINUM(IV), AND RUTHENIUM(III) CEFTRIAXONE DRUG COMPLEXES

Eid H. Alosaimi*

Department of Chemistry, College of Science, University of Bisha, P.O. Box 511, Bisha 61922, Saudi Arabia

(Received December 25, 2023; Revised March 24, 2024; Accepted March 27, 2024)

**ABSTRACT**. Three new metal complexes of ceftriaxone (cef), incorporating platinum(IV), gold(III), and ruthenium(III), were prepared. The complexes were prepared using a 1:2 molar ratio between ceftriaxone sodium salt ($Na_2$cef) to $AuCl_3$, $PtCl_4$, and $RuCl_3$ salts in methanol solvent. The as-synthesized complexes were characterized using microanalytical techniques for C, H, N, and S elements, magnetic and molar conductance measurements, as well as spectroscopic methods including FTIR, $^1$H NMR, and UV-Vis. The shape, morphology and size calculations have been examined using SEM, TEM, and X-ray diffraction data. The cef complexes were six-coordinate systems possessing a distorted octahedral geometry. Through the oxygen of both triazine and carboxylate moieties with the chemical formulae $[Au(cef)_2(Cl)(H_2O)]$ (**I**), $[Pt(cef)_2(Cl)_2]$ (**II**), and $[Ru(cef)_2(Cl)(H_2O)]$ (**III**) the antibiotic cef acts as a bidentate ligand towards three metal ions. The newly created complexes demonstrated antibacterial activity showing efficacy in comparison to the cef sodium ligands. In vitro, antibacterial assays against specific microorganisms were evaluated to assess the antibacterial activities of the complexes. Cytotoxicity assays for cef complexes were conducted for HepG-2 and MCF-7 cell lines, representing human hepatocellular carcinoma and breast cancer, respectively. A value of 22.4 g and 26.2 g for 50% inhibitory concentration ($IC_{50}$), respectively, for HepG-2 and MCF-7 were obtained for $[Ru(cef)_2(Cl)(H_2O)]$ (**III**).

**KEY WORDS**: Ceftriaxone sodium, Gold, Ruthenium, Platinum, Complexes, FTIR, $IC_{50}$

## INTRODUCTION

The chemistry of transition metal complexes has received considerable attention largely due to their catalytic and bioinorganic relevance. Such complexes are also important due to their potential biological activities such as antibacterial, antifungal, antimalarial, and antitumor [1-6]. The third-generation cephalosporin ceftriaxone (cef) was created in the 1980s with antibacterial activity for Gram-negative and Gram-positive strains of bacteria. This activity describes the indications, action, and contraindications for third generation cephalosporins as a valuable agent in the management of gram-negative meningitis, Lyme disease, *Pseudomonas pneumonia*, gram-negative sepsis, *Streptococcal endocarditis*, melioidosis, penicillinase-producing *Neisseria gonorrhea*, chancroid, and gram-negative osteomyelitis [7, 8]. For a variety of diseases, including meningitis, urinary infections, intra-abdominal infections, etc., cef has been used as first-line treatment globally [8-10]. Its efficacy is attributed to the inherent positive traits, such as excellent penetration coupled with the prolonged plasma half-life in diverse bodily fluids like cerebrospinal fluid, and the lack of a requirement in case of renal impairment for dose adjustment [9, 10]. The third-generation cephalosporins include the antibiotic cef. While slightly more active than fourth-generation medicines against Gram-negative germs, third-generation cephalosporins are significantly less effective. Numerous transition metals, acting as pivotal centers within important bioactive compounds in living systems, are recognized for their potent biological effects [11]. Figure 1 demonstrates the chemical structure of cef disodium. It is widely recognized that specific transition metals exert significant biological impact as active centers within living systems. It is

*Corresponding authors. E-mail: ealosaimi@ub.edu.sa

well known that certain transition metals have strong biological influences and operate as active centers in crucial bioactive compounds in living systems [11]. Cef (Rocephin) proves to be an effective treatment for a variety of illnesses, encompassing conditions such as meningitis, acute otitis media, gonorrhea as well as infections affecting the respiratory tract and the skin. Figure 1 depicts the cef disodium structure.

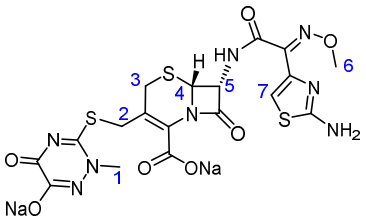

Figure 1. Structure of ceftriaxone sodium salt ($Na_2$cef).

Recent research suggests that cef possesses anti-inflammatory and antioxidant capabilities in liver, kidneys, and brain tissues [12, 13]. It has been reported that cef may reduce lipid peroxidation, inflammation, and oxidative stress to mitigate nephrotoxicity brought on by cadmium [14], cyclosporine [15], tobramycin [16], and isepamicin [17]. Since some transition metals are essential for biological systems and copper(II) among them is critical for cell metabolism and has demonstrated therapeutic value for a range of medical conditions [18, 19]. Metal compounds of cef have pharmacological and toxicological properties [20]. Cef may precipitate in ways that induce serious pharmaceutical side effects upon interaction with metal ions [21]. Pb(II) possesses five coordinates and a warped square pyramidal design. ceftria2- and Pb(II) are coordinated by means of the N and O of the carboxylate, lactam carbonyl, amine and triazine. [Pb(Ceftria)]$3H_2O$ has different antibacterial properties that vary across different bacterial strains. In comparison to cef, for *S. aureus* the antibacterial activity diminishes with negligible activity towards K. pneumoniae. [Pb(Ceftria)]$3H_2O$ exhibits enhanced antibacterial activity against *E. coli*, with a 28% increase at lower concentrations (0.4 mg $mL^{-1}$) compared to cef. However, at concentrations exceeding 0.8 mg $mL^{-1}$, this activity diminishes [22]. Cef hydrated sodium salt ($Na_2$ctx) and Fe(III), Zn(II), Pd(II), Ca(II), and Au(III) metal ions were mixed in a 1:1 M ratio to make five cef antibiotic (ctx) complexes. The Pd(II) and Au(III) complexes possess a coordination number of 4, while Fe(III), Ca(II) and Ca(II), complexes have an octahedral geometry with a coordination number of six. The [Au(ctx)]$Cl_4H_2O$ complex with values of 20.5 and 8.53 g/mL has been shown to have anticancer action against colon carcinoma cells (HCT-116) and hepatocellular carcinoma cells (HepG-2) [23]. To explore the ligating properties of diverse drug moieties, complexes of cef with Co(II), Cu(II), Ni(II) and Fe(II), were synthesized using a ratio of 1:3 ligand to metal. It was discovered that the complexes contained a significant amount of coordinated molecules of water. With the exception of the copper complex, which demonstrated equivalent biological activity against the majority of the tested bacterial strains, the data suggests that the complexes generally exhibit lower biological activity compared to cef. Additionally, moderate biological activity was observed for cef complexes using Fe and Cu transition metals toward *E. coli*, a strain resistant to cef medication [24]. Cef ($H_2$ceftria) interacts to form complexes by interacting with metals(II)such as [M(ceftria)] complexes (M = Co, Cu, Cd, and Mn) and [Fe(ceftria)Cl]. These complexes were subjected to examination for their antibacterial activity against a range of bacteria. The metal complexes of behave differently from cef ligand when used against the same bacteria and inside the same experimental settings. (1) Compared to cef, metal complexes were more effective at destroying bacteria such as *P. aeruginosa* and *P. mirabilis*. (2) Metal complexes demonstrated a lesser effectiveness against *S. aureus* and *S. enteritidis* compared to cef. The Cd(II) complex against *P. mirabilis* exhibited the

most potent antibacterial activity. The iron(III) and antibiotic complexes displayed no effectiveness against *P. aeruginosa*, but the other complexes exhibited effective activity [25]. In the current study, different spectroscopic analytical tools and characterizations such as UV-Vis, FTIR, XRD, $^1$H NMR, SEM, TEM, elemental and thermal analysis for cef complexes of Ru(III), Au(IV) and Pt(IV) were performed. Additionally, all complexes had their antibacterial and anticancer properties assessed.

## EXPERIMENTAL

### *Chemicals and instruments*

The chemicals utilized were highly pure, therefore further purification was not necessary. Sigma-Aldrich Chemical Company (USA) provided the cef sodium, $AuCl_3$, $PtCl_4$, and $RuCl_3$ compounds. The microanalytical analyses of C, H, N, S and halogen contents were carried out using a Perkin Elmer CHN 2400 (USA). The molar conductivities of freshly prepared $10^{-3}$ M dimethylformamide (DMF) solutions were measured for the soluble complexes using Jenway 4010 conductivity meter. The magnetic measurements were performed using magnetic susceptibility balance Sherwood Scientific Cambridge, England. The infrared spectra, as KBr discs, were recorded on a Bruker FT-IR Spectrophotometer (4000–400 $cm^{-1}$). $^1$H-NMR spectra were recorded on Varian Mercury VX-300 NMR spectrometer. The thermal studies were carried out on a Shimadzu TG 50H thermo gravimetric analyzer at a heating rate of 10 ºC $min^{-1}$ under nitrogen till 800 ºC. Scanning electron microscopy (SEM) images were taken in Quanta FEG 250 equipment. The X-ray diffraction patterns were recorded on X 'Pert PRO PAN analytical X-ray powder diffraction, target copper with secondary monochromate. The transmission electron microscopy images (TEM) were performed using JEOL 100s microscopy.

### *Preparations*

By combining 2.0 mmol of $Na_2$cef drug with 1.0 mmol each of $AuCl_3$, $PtCl_4$, and $RuCl_3$ in 50 mL of methanol solvent, three cef complexes were produced. The reaction mixtures were subjected to reflux on a hotplate for approximately 4 hours to generate the colored precipitate. Following cooling, the complexes underwent filtration, were rinsed with hot methanol, dried, and subsequently placed with dry calcium chloride in a desiccator. The product's yield ranged from 82–87% and melting points ranged from 237 to 266 ºC. Table 1 provides a summary of the physical and microanalytical (calc. and found) data for the three synthesized complexes.

Table 1. The physical and microanalytical (calc. and found) data for the three synthesized complexes.

| Complex | Color | Magnetic moment (BM) | Conductance ($ohm^{-1}$ $cm^2$ $mol^{-1}$) | Element | Calc. | Found |
|---|---|---|---|---|---|---|
| $[Au(cef)_2(Cl)(H_2O)]$ (**I**) | Yellow | -- | 27 | %C | 31.90 | 31.33 |
| | | | | %H | 2.53 | 2.46 |
| | | | | % N | 16.53 | 16.00 |
| | | | | %S | 14.19 | 14.32 |
| | | | | %Au | 14.53 | 14.08 |
| $[Pt(cef)_2(Cl)_2]$ (**II**) | Brown | -- | 39 | %C | 31.54 | 31.50 |
| | | | | %H | 2.35 | 2.74 |
| | | | | % N | 16.35 | 16.77 |
| | | | | %S | 14.03 | 14.27 |
| | | | | %Pt | 14.23 | 14.19 |
| $[Ru(cef)_2(Cl)(H_2O)]$ (**III**) | Dark brown | 1.98 | 29 | %C | 34.33 | 34.39 |
| | | | | %H | 2.72 | 2.48 |
| | | | | % N | 17.79 | 17.84 |
| | | | | %S | 15.27 | 15.68 |
| | | | | %Ru | 8.02 | 7.98 |

*Antibacterial and anticancer tests*

The antibiotic resistance for cef and their complexes was examined using a range of bacteria types (*P. aeruginosa*, *B. subtilis*, *S. aureus* and *E. coli*) was checked using filter disc diffusion method [26]. Each substance was dissolved using dimethylsulfoxide (DMSO) to create a solution of concentration $10^{-3}$ M. The paper discs were placed on the Muller Hinton Agar infected solidified medium after being impregnated with 10 L of the chemical concentration. The plates were kept at room temperature for 1 h before being incubated for 24 h at 37 ºC. Thereafter, the measurement of inhibition zones (mm) was conducted. Control discs, containing DMSO, were employed. [27, 28]. The cytotoxic activity using the conventional neutral red uptake assay of Pt(IV), Au(III) and Ru(III) cef complexes was evaluated against MCF-7 cells and HepG-2 cells [29].

## RESULTS AND DISCUSSIONS

*Microanalytical and conductance studies*

The colored metal complexes were synthesized using metal chlorides of Pt(IV), Ru(III) and Au(III) followed by mixing with the sodium salt of cef ($Na_2$cef) ligand in a molar ratio of 2:1. Table 1 shows the complexes colors, chemical analysis results, molar conductance (m = 27-39 $ohm^{-1}$. $cm^2.mol^{-1}$), and magnetic susceptibility values. Based on their chelating behaviors, the Pt(IV), Ru(III) and Au(III) complexes are yellow, brown, and dark brown, respectively. The cef complexes are non-electrolytic characteristics with a 1:2 stoichiometric ratio, according to the molar conductivity data. As a result, complexes **I** – **III** can be expressed as $[Au(cef)_2(Cl)(H_2O)]$ (complex **I**), $[Pt(cef)_2(Cl)_2]$ (complex **II**), and $[Ru(cef)_2(Cl)(H_2O)]$ (complex **III**), respectively (Figure 2). The produced were soluble in DMSO and DMF and insoluble in water, alcohols, $CHCl_3$, $CH_2Cl_2$, and $CCl_4$.

Microanalytical, magnetic, molar conductance, UV-Vis, FTIR, $^1$H NMR, XRD SEM and TEM, investigations were implemented to fully characterize complexes. Ratio 1:2; Metal:cef formulation of all complexes was well supported by the elemental analysis (Figure 2).

*FTIR spectral studies*

FT-IR spectra of the cef complexes $[Au(cef)_2(Cl)(H_2O)]$ (**I**), $[Pt(cef)_2(Cl)_2]$ (**II**), and $[Ru(cef)_2(Cl)(H_2O)]$ (**III**) were assigned to determine the mechanism of coordination of cef sodium towards Pt(IV), Ru(III) and Au(III) metal ions (Figure 3). The functional groups taking part in the coordination have their stretching vibration bands designated (Table 2). The (C=O) triazine and ν(C=O) lactam bands shift towards respective values of 1760, 1634 $cm^{-1}$ and 1610, 1513 $cm^{-1}$ after cef complexes with the metal ions [30]. The changes in the stretching vibrations of carbonyl groups present in both lactam and triazine can be attributed to the coordination of oxygen atoms for metal ions with chelating complexes. The carboxylate group's symmetric stretching frequencies shift to 1363–1344 $cm^{-1}$ [30]. The band for ν(NH) stretching vibration ($-NH_2$) at 3200 $cm^{-1}$, remains unchanged. This observation confirms nonparticipation of the amino group nitrogen atom with metal ions, according to the FTIR spectrum frequencies for $Na_2$cef and its three complexes (**I-III**). A disparity surpassing 200 $cm^{-1}$ serves as an indication of monodentate coordination, whereas it is a bidentate coordination mode if the variance is < 200 $cm^{-1}$, according to Deacon and Phillips' classifications and carboxylate group coordination behavior [30]. The coordination is monodentate in the synthesized cef complexes (**I-III**), substantiated by the observation that the difference between ν(asym) and ν(sym) is 200 $cm^{-1}$. The coordination is facilitated by the oxygen of the carboxylate group (COO) and the oxo group of the triazine ring,

as indicated by these shifts. The vibration bands ν(MO) (MN) account for the emergence of new frequency modes in the range of 600 to 400 $cm^{-1}$ in these complexes.

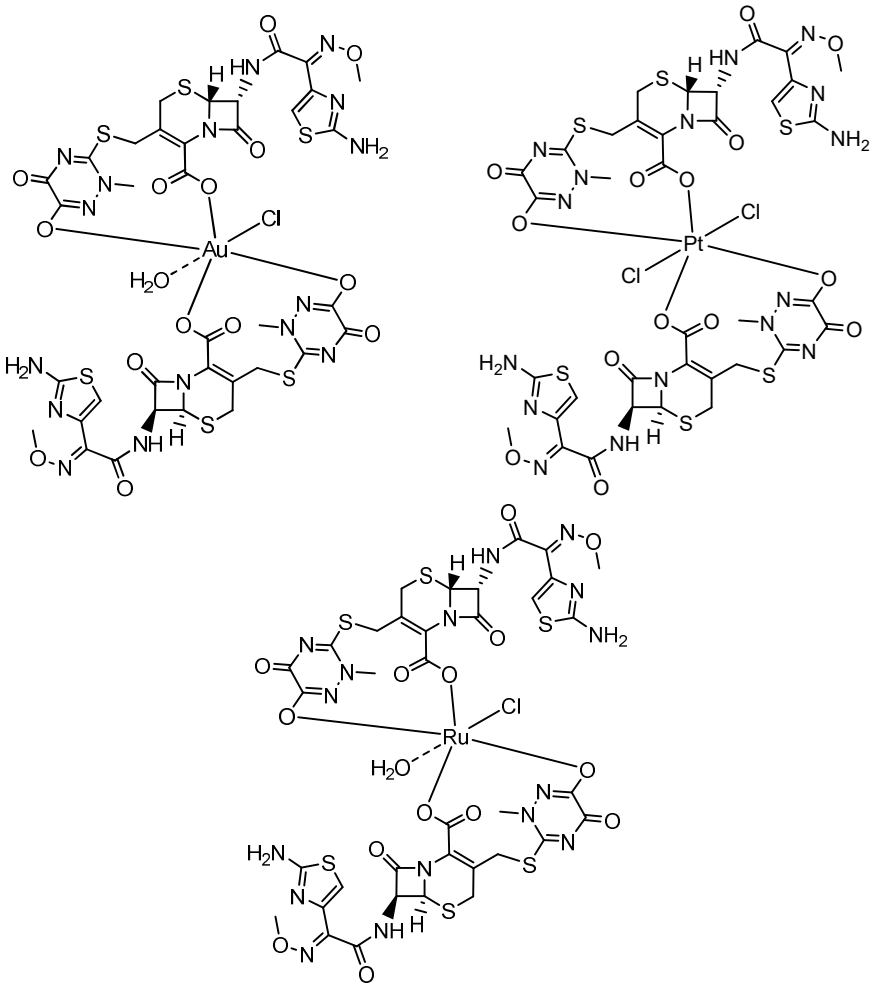


Figure 2. Speculated structures of complexes **I**, **II**, and **III**.

*Magnetic and electronic spectra studies*

The C=O, C=C, and C=N chromophoric groups induce π-π* transitions and contribute to the cef sodium salt-free ligand's maximum wavelength at 290 nm. The variance in wavelength data among complexes I–III may arise not from the intrinsic properties of the ligand but rather from the interaction of metal ions with the ligand, resulting in metal complex formation [31]. The complexes spectral bands underwent a bathochromic shift to higher values, and the emergence of new absorption bands suggested complex formation [32]. Moreover, the complexes display bands in the 316–419 nm region, indicative of ligand-to-metal charge transfer [23]. The Ru(III) complex

estimated magnetic moment is eff = 1.98 B.M., which agrees well with the geometry in the six-coordinate system [23].

Table 2. Infrared spectral data ($cm^{-1}$) of $Na_2cef$ and complexes **I-III**.

| Compounds | | | | Assignments |
|---|---|---|---|---|
| $Na_2cef$ | Au(III) | Pt(IV) | Ru(III) | |
| 3200 | 3195 | 3194 | 3194 | ν(N–H); $NH_2$ |
| 1746 | 1693 | 1634 | 1760 1669 | ν(C=O) of amide and β–lactam |
| 1605 | 1571 | 1550 | 1610 1533 | $\nu_{as}$ $(C–N)_{triazine}$ + $\nu_{as}(COO)$ + $\nu(C=O)_{oxo}$ |
| 1403 | 1406 | 1436 | 1436 | $\delta(CH_2)$ + $\delta(CH_3)$ |
| 1367 | 1363 | 1344 | 1363 | $\nu_s(COO)$ + δ(CH) of β–lactam |
| 1287 | 1310 | - | 1291 | $\nu_s$(C–N) of triazine |
| 1244 | 1242 | 1247 | 1203 | $\delta_w(CH_3)$ + δ(CH) of β–lactam |
| 1187 | 1188 | 1102 | 1106 | $\delta_r(CH_3)$ |
| 1036 | 1039 | 1034 | 1039 | δ(CH) aminothiazole |
| 891 | 874 | 801 | 889 | ν(N–O) methoxy |
| - | 583, 559<br>457, 424 | 598, 559<br>462, 424 | 642, 510<br>460, 432 | ν(M–O) + ν(M–N) |

*$^1$H-NMR study*

The $^1$HNMR spectra of free $Na_2cef$ ligand (400 MHz, DMSO-$d_6$): δ 3.498 [3H, N-$CH_3$ of triazine ring], 3.952 [2H, S–$CH_2$], 5.659 [1H, β–lactam], 5.072 [1H, β–lactam], 3.374 and 3.584 [2H, $CH_2$ of thiazine], 3.893 [3H, =N-O-$CH_3$] and 6.885 [1H, of thiazol ring]. Referring to the $^1$H-NMR spectra of the $[Au(cef)_2(Cl)(H_2O)]$ (**I**) and $[Pt(cef)_2(Cl)_2)$ (**II**) complexes (Table 3), upfield shifts were identified in the signals of the $Na_2cef$ ligand. These shifts were indicative of chelation among Au(III) and Pt(III) with the ligand.

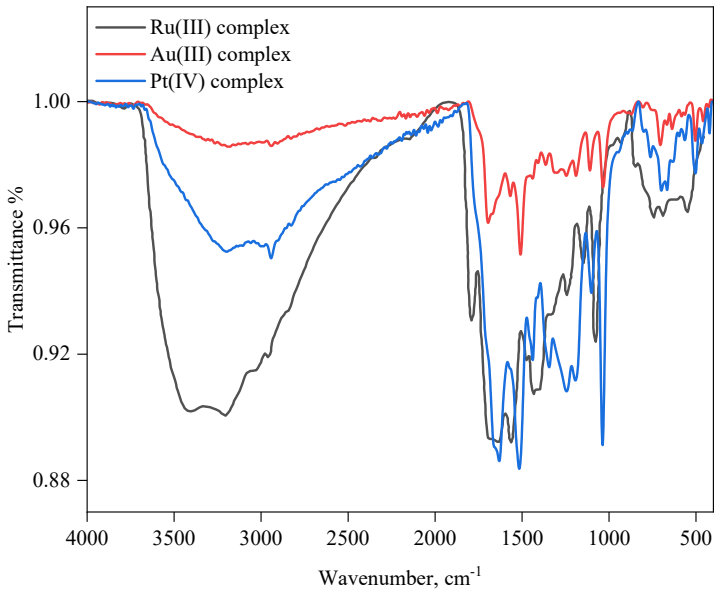


Figure 3. FTIR spectra of complexes **I**, **II**, and **III**.

Table 3. $^1$H NMR spectral data (ppm) of $Na_2$cef, gold(III) and platinum(IV) complexes.

| Assignments, carbon atom number | Compounds | | |
|---|---|---|---|
| | $Na_2$ctx | Au(III) | Pt(IV) |
| 1 | 3.498 | 3.591 | 3.586 |
| 2 | 3.952 | 3.956 | 3.956 |
| 3 | 3.374, 3.584 | 3.370, 3.770 | 3.366, 3.573 |
| 4 | 5.072 | 5.100 | 5.086 |
| 5 | 5.659 | 5.712 | 5.811 |
| 6 | 3.893 | 3.882 | 3.882 |
| 7 | 6.885 | 7.254, 7.375, 7.481 | 7.274, 7.376, 7.478 |

*Morphological analysis*

The XRD patterns of $[Au(cef)_2(Cl)(H_2O)]$ (**I**), $[Pt(cef)_2(Cl)_2]$ (**II**) and $[Ru(cef)_2(Cl)(H_2O)]$ (**III**) have been demonstrated. Within the 2θ range spanning 2-80°, the diffraction patterns display characteristics of amorphous behavior, accompanied by a nano-structural appearance. The Scherrer relationship [23] was used to compute the particle size at full width at half-maximum (FWHM) measurements, with a resulting nano-size range. SEM images of the Ru(III), Pt(IV), and Au(III) complexes at an energy of 30 kV and a magnification of x 5,00 to 10,000, were acquired. The SEM image of complexes depict the aggregation and uniform homogeneity. The transmission electron microscopy (TEM) technique for the complexes $[Au(cef)_2(Cl)(H_2O)]$ (I), $[Pt(cef)_2(Cl)_2]$ (**II**), and $[Ru(cef)_2(Cl)(H_2O)]$ (**III**), Black and spherical spots representing nanoparticles within 20–40 nm range.

*Thermal analysis*

TG studies were conducted to determine the structures of the $[Au(cef)_2(Cl)(H_2O)]$ (**I**), $[Pt(cef)_2(Cl)_2)$ (**II**) and $[Ru(cef)_2(Cl)(H_2O)]$ (**III**) complexes under an inert nitrogen environment at 10 $^oC\ min^{-1}$ (Figure. 4). Three decomposition phases were observed for the $[Au(cef)_2(Cl)(H_2O)]$ (**I**) complex during thermal decomposition. At maximum temperatures of 242, 326, and 757 $^oC$, the gold(III) complex undergoes mass losses, accounting for a total weight reduction of 37.86%. This reduction corresponds to the loss of $H_{34}ClN_{16}O_{15}$ species. The ultimate thermal decomposition product acquired is Au(metal) + organic moiety (62.14%), as a residual solid material. There are three stages of thermal degradation at 134, 231, and 362 which are visible in the $[Pt(cef)_2(Cl)_2)]$ (**II**) complex's thermal decomposition curve due to lost $C_{22}H_{32}C_{l2}N_{16}O_{12}$ organic moiety. The final thermal breakdown product obtained is $PtO_2$ + organic moiety (43.31%). Similarly, for$[Ru(cef)_2(Cl)(H_2O)]$ (**III**) complex, the obtained final thermal decomposition product is $RuO_2$ + organic moiety (72.96%), after three degradation steps and a weight loss (27.04%) equal to the loss of $H_{34}ClN_4O_{13}$ organic species.

*Antibacterial activity*

The biological potential of the $[Au(cef)_2(Cl)(H_2O)]$ (**I**), $[Pt(cef)_2(Cl)_2)$ (II), and $[Ru(cef)_2(Cl)(H_2O)]$ (**III**) complexes was tested using different bacterial strains. According to the results presented in (Table 4), newly synthesized complexes exhibit measurable bactericidal action, and this activity was enhanced upon complexation with metal ions. The newly synthesized complexes underwent an assessment of their biological activity relative to all substances and compared to ampicillin as an antibacterial agent against all the examined species. The inhibitory order for the strains was as follows: For *B. subtilis*: Ampicillin > Pt(IV) > Ru(III) > Au(III), for *S. aureus:* Ampicillin > Pt(IV) > Au(III) = Ru(III), , for *E. coil*: Ampicillin > Pt(IV) > Au(III) = Ru(III), for *P.aeruginosa:* Ampicillin > Pt(IV) > Au(III) = Ru(III). Based on the findings, the

remarkable antibacterial activity of metal complexes has been evident. This fact corresponds to the chelation theory, where chelation helps and enables the complex to pass through a pathogen's cell membrane, diffuse in the spore membrane lipid layer and ultimately cause its death [23-25]. According to the results, the activity of gold(III) or platinum(IV) complexes has been dramatically changed by the Ru(III) complex.

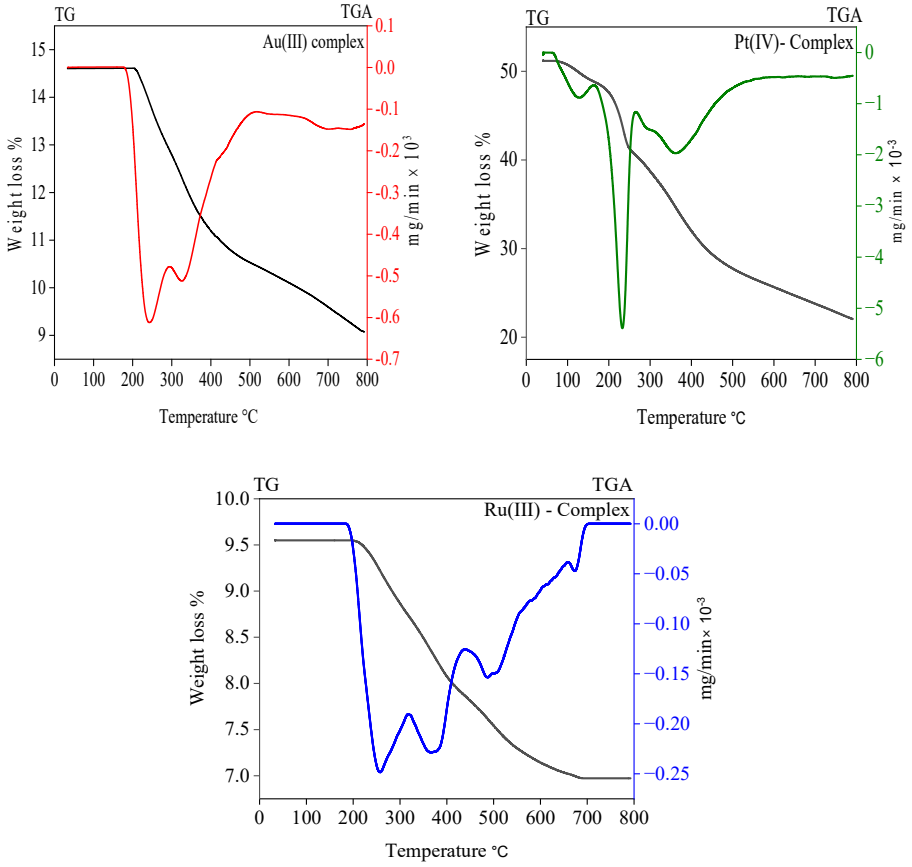


Figure 4. TGA/DTG diagrams of cef complexes.

*Anticancer activity*

Using the conventional neutral red uptake assay method, the cytotoxicity of the $[Au(cef)_2(Cl)(H_2O)]$ (I) (HepG-2 = 60.6 g/mL & MCF-7 = 53.4 g/mL), $[Pt(cef)_2(Cl)_2)$ (II) (HepG-2 = 51.2 g/mL and MCF-7 = 61.7 g/mL), and $[Ru(cef)_2(Cl)(H_2O)]$ (III) (HepG-2 = 22.4 g/mL and MCF-7 = 26.2 g/mL) complexes for the cancer cell cultures namely HepG-2 and MCF-7 cells was evaluated (Figures 5 and 6). Considering the 50% inhibitory concentrations of cellular viability ($IC_{50}$) values of the three prepared complexes, we find that the ruthenium(III) complex has a higher activity (HepG-2 = 22.4 g/mL and MCF-7 = 26.2 g/mL) compared to both the gold and platinum compounds.

Table 4. Antibacterial activity values of the synthesized cef compounds.

| Sample | Diameters of inhibition zones (mm/mg sample) | | | |
|---|---|---|---|---|
| | Bacterial species $G^+$ | | Bacterial species $G^-$ | |
| | *B. subtilis* | *S. aureus* | *E. coli* | *P. aeruginosa* |
| Control: DMSO | 0.0 | 0.0 | 0.0 | 0.0 |
| Standard: Ampicillin antibacterial agent | 26 | 21 | 25 | 26 |
| Au(III) | 9 | 9 | 10 | 10 |
| Pt(IV) | 14 | 18 | 14 | 15 |
| Ru(III) | 10 | 9 | 10 | 10 |

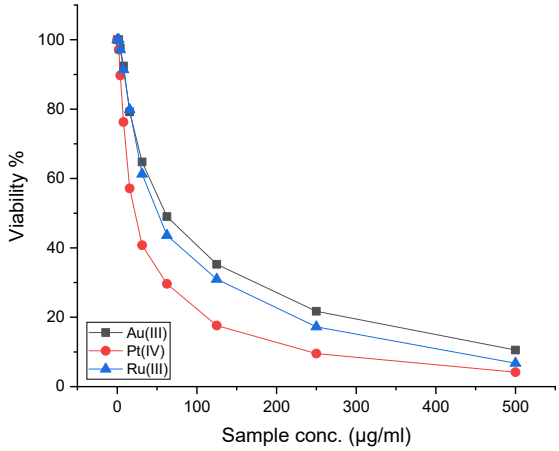


Figure 5. Viability (%) of the human hepatocellular carcinoma HepG-2 cells treated with Au(III), Pt(IV), and Ru(III) cef complexes at different concentrations.

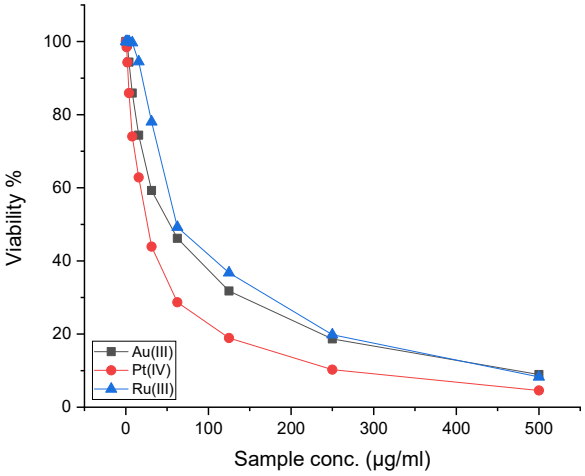


Figure 6. The viability (%) of the human breast cancer cell line MCF-7 cells was assessed after treatment with various concentrations of cef complexes with Au(III), Pt(IV), and Ru(III).

## CONCLUSION

The objective of this paper was to synthesize three novel cef complexes by reacting cef sodium salt with salts of $AuCl_3$, Pt(IV), and $RuCl_3$ in methanol. The structures of the prepared cef complexes were investigated by molar conductance, microanalytical and magnetic analysis, UV-Vis, FTIR, $^1$HNMR, SEM, TEM and XRD. A distorted octahedral behavior is created by the cef ligand modeling as a bidentate ligand. The distorted octahedral geometry is induced by the cef ligand, which functions as a bidentate ligand. All synthetic complexes were coordinated by the triazine's and the carboxylate's oxygen atoms. The $[Ru(cef)_2(Cl)(H_2O)]$ (**III**) complex displays anticancer activity against MCF-7 and HepG-2 and with 50% inhibitory concentrations of cellular viability (IC50) of 22.4 g/mL and 26.2 g/mL, respectively.

## ACKNOWLEDGMENT

The authors are thankful to the Deanship of Graduate Studies and Scientific Research at University of Bisha for supporting this work through the Fast-Track Research Support Program.

## REFERENCES

1. Abdel Majid, A.A.; Moamen, S.R.; Ahmed, G.; Ivo, G. Complexation of alkaline earth metals $Mg^{2+}$, $Ca^{2+}$, $Sr^{2+}$ and $Ba^{2+}$ with adrenaline hormone: Synthesis, spectroscopic and antimicrobial analysis. *Bull. Chem. Soc. Ethiop*. **2023**, 37, 357-372.
2. Ayman, A.O.Y. Synthesis, biological evaluation and molecular docking studies of novel mixed-ligand Schiff base/8-hydroxyquinoline metal complexes. *Mater. Express*. **2023**, 13, 2110-2127.
3. Amnah, M.A.; Abdel Majid, A.A.; Moamen, S.R.; Mohamed, I.K.; Safyah, B.B.; Eman, S.B. Spectroscopic, thermal, and anticancer investigations of new cobalt(II) and nickel(II) triazine complexes. *Bull. Chem. Soc. Ethiop*. **2022**, 36, 363-372
4. Amnah, M.A.; Abdel Majid, A.A.; Moamen, S.R. Four new tin(II), uranyl(II), vanadyl(II), and zirconyl(II) alloxan biomolecule complexes: synthesis, spectroscopic and thermal characterizations. *Bull. Chem. Soc. Ethiop*. **2022**, 36, 373-385.
5. Ayman, A.O.Y.; Moamen, S.R.; Hosam, A.S.; Abdel Majid, A.A.; Omar, M.A.; Ghayah, M.A.; Amnah, M.A. Complexation of some alkaline earth metals with bidentate uracil ligand: Synthesis, spectroscopic and antimicrobial analysis. *Bull. Chem. Soc. Ethiop*. **2022**, 36, 373-385
6. Ayman, A.O.Y.; Amnah, M.A.; Moamen, S.R. Preparation, spectroscopic and thermal studies on the zinc(II), cadmium(II), tin(II), lead(II) and antimony(III) creatinine complexes. *Bull. Chem. Soc. Ethiop*. **2022**, 36, 831-842.
7. Reiner, R.; Weiss, U.; Brombacher, U.; Lanz, P.; Montavon, M.; Furlenmeier, A.; Angehrn, P.; Probst, P. J. RO 13-9904/001, a novel potent and long-acting parenteral cephalosporin. *J. Antibiotics* **1980**, 33, 783-786
8. Fernandes, R.; Amador, P.; Prudêncio, C. β-Lactams, chemical structure, mode of action and mechanisms of resistance. *Rev. Mod. Microbiol*. **2013**, 24, 7-17.
9. Heather, M.O. ; Alekha, K.D. Ceftriaxone sodium: comprehensive profile. *Profiles Drug Subst. Excip. Relat. Methodol*. **2003**, 30, 21-57.
10. Yazed, S.A.; Gregorio, B.; Khalid, B.S.; Thamer, A.A.; Fadi, S.; Eleftherios, M. Effectiveness and safety of ceftriaxone compared to standard of care for treatment of bloodstream infections due to methicillin-susceptible *Staphylococcus aureus*: A systematic review and meta-analysis. *Antibiotics* **2022**, 11, 375.

11. Aleksandr, O.L.; Galina, V.N.; Alexander, A.K.; Natalia, A.S.; Natalia, I.S.; Sergey, A.V.; Pavel, O.K. A complex of ceftriaxone with Pb(II): Synthesis, characterization, and antibacterial activity study. *J. Coord. Chem*. **2014**, 67, 2783-2794.
12. Abdel-Daim, M.M.; Aleya, L.; El-Bialy, B.E.; Abushouk, A.I.; Alkahtani, S.; Alarifi, S.; Alkahtane, A.A.; AlBasher, G.; Ali, D.; Almeer, R.S.; Al-Sultan, N.K.; Alghamdi, J.; Alahmari, A.; Simona G Bungau, S.G. The ameliorative effect of ceftriaxone and vitamin E against cisplatin-induced nephrotoxicity. *Environ. Sci. Pollut. Res. Int*. **2019**, 26, 15248-15254.
13. Hakimizadeh, E.; Kaeidi, A.; Taghipour, Z.; Mehrzadi, S.; Allahtavokoli, M.; Shamsizadeheh, A.; Bazmandegan, G.; Hassanshahi, J.; Aflatoonian, M.R.; Fatemi, I. Ceftriaxone improves senile neurocognition damages induced by D-galactose in mice. *Iran J. Basic Med. Sci*. **2020**, 23, 368-375.
14. Vivek, K.D.; Anuj, B.; Manu, C. Protective role of ceftriaxone plus sulbactam with VRP 1034 on oxidative stress, hematological and enzymatic parameters in cadmium toxicity induced rat model. *Interdiscip. Toxicol*. **2012**, 5, 192-200.
15. Nigar, Y.; Selçuk, I.; Nazıroğlu, M.; Süleyman, O.; Ahmet, N.; Vefik, A.; Murat, T. Ceftriaxone ameliorates cyclosporine A-induced oxidative nephrotoxicity in rat. *Cell Biochem. Funct*. **2011**, 29, 102-107.
16. Beauchamp, D.; Thériault, G .; Grenier, L .; Gourde, P .; Perron, S .; Bergeron, Y .; Fontaine L.; Bergeron, M.G. Ceftriaxone protects against tobramycin nephrotoxicity, *Antimicrob. Agents Chemother*. **1994**, 38, 750-756.
17. Yoshiyama, Y.; Yazaki, T.; Beauchamp, D.; Kanke, M. Protective effect of ceftriaxone against the nephrotoxicity of isepamicin administered once daily in rats. *Biol. Pharm. Bull*. **1998**, 21, 520-523.
18. John, R.J.S. Copper complexes offer a physiological approach to treatment of chronic diseases. *J. Med. Chem*. **1976**, 19, 135.
19. Binesh, K.; Jai, D.; Anju, M. Synthesis, structure elucidation, antioxidant, antimicrobial, anti-inflammatory and molecular docking studies of transition metal(II) complexes derived from heterocyclic Schiff base ligands. *Res. Chem. Intermed.* **2023,** 49, 2455-2493.
20. Elsayed, M.A.; Mowafak, M.M.; Sherine, E.S. A physical-chemical study of the interference of ceftriaxone antibiotic with copper chloride salt. *Bioinorg. Chem. Appl*. **2021**, 2021, 1-15.
21. Hans-Rudolf, S .; Pascal, D.; Theo, B.; André, B.; Benjamin, G.; Jörg, H. In vitro assessment of the formation of ceftriaxone-calcium precipitates in human plasma. *J. Pharm. Sci*. **2011**, 100, 2300.
22. Aleksandr, O.L.; Krasnoyarsk, R.; Galina, V.N.; Alexander, A.K.; Natalia, A.S.; Natalia, I.S. Sergey, A.V.; Pavel, O.K. A complex of ceftriaxone with Pb(II): Synthesis, characterization, and antibacterial activity study. *J. Coord. Chem*. **2014**, 67, 2783-2794.
23. Refat, M.S.; Altalhi, T.; Fetooh, H.; Alsuhaibani, A.M.; Hassan, R.F. In neutralized medium five new Ca(II), Zn(II), Fe(III), Au(III) and Pd(II) complexity of ceftriaxone antibiotic drug: Synthesis, spectroscopic, morphological and anticancer studies. *J. Mol. Liq*. **2020**, 322, 114816.
24. Alaa, E.A. Synthesis, spectral, thermal and antimicrobial studies of some new tri metallic biologically active ceftriaxone complexes. *Spectrochim. Acta Part A* **2011**, 78, 224-230.
25. Juan, R.A.; Alfreisa, R. Synthesis and antibacterial activity of ceftriaxone metal complexes. *Trans. Met. Chem*. **2005**, 30, 897-901.
26. Julia, H.B.N.; Raphael, E.F.P.; Alexandre, C.; Wilton, R.L.; Pedro, P.C. Silver complexes with sulfathiazole and sulfamethoxazole: Synthesis, spectroscopic characterization, crystal structure and antibacterial assays. *Polyhedron* **2015**, 85 437-444.
27. Imane, H .; Rafika, B.; Chahrazed, T.; Fadila, B.; Mouna, S.; Belkacem, B.; Mhamed, B.; Hocine, M.; Sofiane, B. Synthesis, structure characterization, spectral properties, DFT

calculations, hirshfeld surface analysis, thermal stability and bioactivity of a new sulfamethoxazole zinc(II) complex. *J. Mol. Struct*. **2022,** 1261, 132962
28. Sanjay, M.T.; Urmila, H.P. Synthesis, spectroscopic characterization, antimicrobial activity and crystal structure of $[Ag_2(C_{10}H_{10}N_3O_3S)_2(C_5H_5N)_3]$. *J. Mol. Struct*. **2015**, 1088, 161-168.
29. Guillermo, R.; Ana, d.P.; Jorge, L.Z. Neutral red uptake assay for the estimation of cell viability/cytotoxicity. *Nature Protocols* **2008**, 3, 1125-1131.
30. Kazuo, N. *Infrared and Raman Spectra of Inorganic and Coordination C*ompounds, 4th ed., John Wiley and Sons: New York; **1986**; p 250.
31. Lever, A.B.P. *Electronic Spectra of* $d^n$ *Ions Inorganic Electronic Spectroscopy*, 2nd ed., John Wiley and Sons: New York; **1984**; p 180.
32. Albert, C.F.; Geoffrey, W. *The Element of First Transition Series Advanced Inorganic Chemistry*, 3rd ed., John Wiley and Sons: New York; **1992**; p 458.